Enhanced Peroxynitrite Formation Is Associated with Vascular Aging

By Bernd van der Loo,*‡ Ralf Labugger,‡ Jeremy N. Skepper,§ Markus Bachschmid,‖ Juliane Kilo,*‡ Janet M. Powell,§ Miriam Palacios-Callender,¶ Jorge D. Erusalimsky,¶ Thomas Quaschning,‡ Tadeusz Malinski,** Daniel Gygi,‡ Volker Ullrich,‖ and Thomas F. Lüscher*‡

*From the *Division of Cardiology, University Hospital, 8091 Zurich, Switzerland; the ‡Division of Cardiovascular Research, Institute of Physiology, University Zurich-Irchel, 8057 Zurich, Switzerland; the §Multi-Imaging Centre, University of Cambridge, Cambridge CB2 3DY, United Kingdom; the ‖Department of Biology, University of Konstanz, 78434 Konstanz, Germany; the ¶Wolfson Institute for Biomedical Research and the Department of Medicine, University College London, London WC1E 6JJ, United Kingdom; and the **Department of Chemistry, Institute of Biotechnology, Oakland University, Rochester, Michigan 48309*

Abstract

Vascular aging is mainly characterized by endothelial dysfunction. We found decreased free nitric oxide (NO) levels in aged rat aortas, in conjunction with a sevenfold higher expression and activity of endothelial NO synthase (eNOS). This is shown to be a consequence of age-associated enhanced superoxide ($\cdot O_2^-$) production with concomitant quenching of NO by the formation of peroxynitrite leading to nitrotyrosilation of mitochondrial manganese superoxide dismutase (MnSOD), a molecular footprint of increased peroxynitrite levels, which also increased with age. Thus, vascular aging appears to be initiated by augmented $\cdot O_2^-$ release, trapping of vasorelaxant NO, and subsequent peroxynitrite formation, followed by the nitration and inhibition of MnSOD. Increased eNOS expression and activity is a compensatory, but eventually futile, mechanism to counter regulate the loss of NO. The ultrastructural distribution of 3-nitrotyrosyl suggests that mitochondrial dysfunction plays a major role in the vascular aging process.

Key words: vascular aging • superoxide • nitric oxide • 3-nitrotyrosine • vascular endothelium

Introduction

Cardiovascular diseases increase in frequency with age, even in the absence of established risk factors (1). This suggests that aging by itself alters vascular function. The endothelium exerts a multimodal regulation of vascular smooth muscle tone and structure by the release of nitric oxide (NO),[1] endothelium-derived hyperpolarizing factor, and prostacyclin. NO is generated from L-arginine catalyzed by NO synthases (2, 3). One of these isoenzymes, endothelial NO synthase (eNOS), is constitutively expressed in endothelial cells (4). This enzyme is largely membrane associated as a result of NH_2-terminal myristoylation (5), a reaction which regulates enzymatic biological activity (6, 7).

Endothelium-dependent relaxation declines with increasing age (8). The underlying cellular and molecular mechanisms associated with age-related endothelial dysfunction have not been elucidated, but might involve: (a) changes in expression and/or activity of eNOS (9), (b) increased breakdown of NO due to an augmented production of superoxide anions ($\cdot O_2^-$ [10]), or (c) a gradual loss of antioxidant capacity (11), which normally provides cellular protection against reactive oxygen species.

The role of the L-arginine/NO pathway in the pathophysiology of vascular aging is controversial. Both reduced levels of eNOS mRNA (12) and increased eNOS enzyme expression combined with reduced activity (9) have been reported. Therefore, our first aim was to clarify whether

T. Malinski's present address is the Department of Chemistry and Biochemistry, Ohio University, Athens, OH 45701.

Address correspondence to Thomas F. Lüscher, University Hospital Zurich, Cardiology, Raemistrasse 100, 8091 Zurich, Switzerland. Phone: 41-1-255-2121; Fax: 41-1-255-4251; E-mail: cardiotfl@gmx.ch

[1]*Abbreviations used in this paper:* eNOS, endothelial NOS; iNOS, inducible NOS; MnSOD, manganese superoxide dismutase; NO, nitric oxide; NOS, NO synthase; SNP, sodium nitroprusside; TBS, Tris-buffered saline.

age-associated endothelial dysfunction is causally related to alterations of the L-arginine/NO system. To this end, molecular analyses of eNOS expression and its subcellular localization, which might affect the biological activity of this enzyme system, were performed in aortas from young (4–6 mo), middle-aged (19 mo), and old (32–35 mo) rats and correlated to direct measurements of NO production and vascular function.

Reactive oxygen species and especially $\cdot O_2^-$ are important modulators of NO activity under various pathophysiological conditions (13) and are thought to be involved in the aging process (14). In this context it seemed essential to assess the role of $\cdot O_2^-$, which might scavenge NO to form the powerful oxidant peroxynitrite (15, 16). In vivo generation of peroxynitrite has not been directly demonstrated to date (16). Unlike $\cdot O_2^-$ (pK 4.8), peroxynitrite (with a pK of 6.8) can easily penetrate cells in the protonated form because of its high diffusibility across phospholipid membranes (17). Peroxynitrite is known to initiate oxidative modification of proteins, including the nitration of aromatic rings (18), sulfoxidation of methionin, and *S*-nitrosylation of cysteine followed by disulfide formation, thereby rendering inactive certain functionally important regulatory proteins, like receptors or enzymes (19). Nitration of tyrosine is the underlying mechanism of prostacyclin synthase inhibition by peroxynitrite (20). Evidence for the in vivo formation of peroxynitrite has been derived from immunohistochemical detection of nitrotyrosine in human atherosclerotic lesions (21) and in the tissue of rejected human renal allografts (22). Recent indirect evidence (23) suggests that specific enzymes may selectively accumulate oxidative damage during aging. This is supported by a recent study demonstrating increased nitration of the sarcoplasmic reticular Ca-ATPase isolated from the skeletal muscle of 28-mo-old F344 rats (24).

Our second aim was to test the hypothesis that increased nitration of protective, antioxidant enzymes, leading to their inactivation with age, might be a contributing molecular pathway for oxidative damage to vascular tissue. We will show that the reduced endothelium-dependent relaxation associated with aging is not due to downregulation of eNOS but rather to increased inactivation of NO by $\cdot O_2^-$ entailing altered NO bioavailability, as NO is removed through the formation of peroxynitrite. The evidence for a close association between the formation of peroxynitrite and age-associated vascular endothelial dysfunction provided in this study is further strengthened by the demonstration of a selective nitration of manganese superoxide dismutase (MnSOD) with increased age. The paradoxical increase in eNOS expression and activity appears to be a compensatory mechanism attempting to counteract increased NO inactivation by $\cdot O_2^-$.

Materials and Methods

Materials

Acetylcholine chloride, calcium ionophore A23187, sodium nitroprusside (SNP), and N^G-monomethyl-L-arginine (L-NMMA) were all from Sigma-Aldrich. L-[^{14}C]arginine was purchased from Amersham Pharmacia Biotech and tetrahydrobiopterin from Schircks Laboratories.

Animals

F1 (F344 × BN) healthy male rats, fed ad libitum, were obtained from the National Institutes of Health, National Institute on Aging (Bethesda, MD). The colonies are maintained under contractual arrangement with Harlan Sprague Dawley, Inc. All studies were performed in three different age groups: 4–6-mo-old ("young"), 19-mo-old ("middle-aged"), and 32–35-mo-old ("old") rats. Heart rate and systolic arterial blood pressure were measured in conscious animals using the tail-cuff method with a custom-made pulse pressure transducer, and the mean of five independent determinations was calculated.

Surgical Procedures

On the day of the experiment, rats were anesthetized with ketamine (1 ml/kg body wt) and xylazine (0.5 ml/kg bw; E. Gräub AG). To avoid intravascular clotting, a bolus of 5,000 IU heparin was given before surgery. The chest and abdomen were opened with a medial sternotomy, and the entire aorta from the heart to the iliac bifurcation was excised and placed in cold (4°C) Krebs-Ringer bicarbonate solution. The isolated aorta was cleaned of adhering tissue under a dissection microscope (model M3C; Wild AG).

All studies were performed on corresponding anatomical sites of the aorta from each animal (unless otherwise stated, $n = 8$ for young and old rats, $n = 7$ for middle-aged rats). All of the procedures and experimental protocols were approved by the local authorities for animal research (Commission for Animal Research of the Canton of Zurich, Switzerland).

Organ Chambers

Rings of aorta 4–5 mm long were horizontally mounted between two stirrups in organ chambers filled with Krebs-Ringer bicarbonate solution (pH 7.4, 37°C, 95% O_2; 5% CO_2) of the following composition: NaCl (118.6 mmol/liter), KCl (4.7 mmol/liter), $CaCl_2$ (2.5 mmol/liter), KH_2PO_4 (1.2 mmol/liter), $MgSO_4$ (1.2 mmol/liter), $NaHCO_3$ (25.1 mmol/liter), glucose (11.1 mmol/liter), calcium EDTA (0.026 mmol/liter). Isometric tension was recorded continuously. After a 30-min equilibration period, rings were gradually stretched (2 *g*) until the optimal tension–length relationship was reached as determined by the contraction to KCl (100 mmol/liter). Before the start of the experiments, rings were allowed to equilibrate for another 30 min. Vessels were preconstricted with 2–5 × 10^{-7} mol/liter norepinephrine until a stable plateau of ~70% of the contractile response to KCl was reached. For endothelium-dependent relaxation, vessels were then relaxed with acetylcholine (10^{-10}–10^{-4} mol/liter) or calcium ionophore A23187 (10^{-10}–10^{-6} mol/liter). SNP (10^{-10}–10^{-5} mol/liter) was used as an endothelium-independent agonist.

Porphyrinic NO Microsensor

Direct in situ measurements of NO were carried out using a three-electrode system: a porphyrinic NO microsensor as the working electrode (anode), a platinum wire auxiliary electrode (cathode), and a standard calomel reference electrode (8, 25). Amperometric mode detection was used at a constant potential, equal to the peak potential for NO oxidation of the working electrode. The signal was detected in a current range of 10 μA with a pulse height of 50 mV and a drop time of 0.5 s. The amperometric signal was recorded with a Kipp & Zonen chart recorder (Recom Electronic AG). Standard NO solutions (1.8

mmol/liter) were prepared from an aqueous solution saturated with pure NO gas (Garbagas), and NO concentrations were calculated using a calibration curve with an NO standard. Immediately before NO measurements, aortic rings of 3–4 mm length were cut longitudinally and pinned on the bottom of an organ chamber filled with fresh, phenol red–free, HBSS buffer (37°C, pH 7.40). Then the active tip of the L-shaped porphyrinic NO microsensor was placed on the endothelial surface using a precision stereo zoom microscope and a micromanipulator M3301 (World Precision Instruments). For maximal stimulation of eNOS, calcium ionophore A23187 was injected into the organ bath to yield a final concentration of 10^{-6} mol/liter. A mean of at least two independent determinations on two adjacent sections was calculated for each animal.

Measurement of Superoxide

$\cdot O_2^-$ concentration in aortic tissue was determined using a lucigenin enhanced chemiluminescence method (26, 27). Each tissue sample (5 mm length) was placed into 500 μl modified Krebs-Ringer solution, pH 7.40, and prewarmed to 37°C for 1 h. Immediately before measurement, rings were transferred into scintillation vials filled with 500 μl Krebs-Hepes solution, pH 7.40, at room temperature. 12.5 μl lucigenin (bis-*N*-methylacridinium nitrate; Sigma-Aldrich) was added to give a final concentration of 250 μmol/liter. $\cdot O_2^-$-generated chemiluminescence of lucigenin was detected with a scintillation counter (Raytest PW 4700; Philips) connected to a Philips personal computer system. The computer was programmed to measure $\cdot O_2^-$ in defined time intervals. $\cdot O_2^-$ production by the tissue was calculated as the mean of those last five values that did not differ by >5% from each other and was expressed as counts/(min × mg tissue). For maximal stimulation, rings were incubated with 10^{-6} mol/liter calcium ionophore A23187. In some vessels, the endothelium was mechanically removed 30 min before the experiment. All measurements were performed on two or three aortic rings for each animal, and the mean was calculated.

Determination of Total eNOS Protein Expression

For extraction of endothelial cells, a 1.5-cm-long segment of freshly taken aorta was cut longitudinally and fixed on a gelatinated dish. The aorta was washed with RPMI medium (GIBCO BRL), then incubated with collagenase at 37°C for 15 min, and finally the endothelium was scraped off with a surgical blade. After centrifugation at 5,000 rpm and 4°C for 5 min, the pellet was homogenized in 100 μl Tris-SDS (2%) buffer followed by a 15-min incubation on ice, a 1-min sonication in a water bath, and subsequent boiling. Protein concentrations in the lysates were measured using the bicinchoninic acid (BCA) Protein Assay Kit (Pierce Chemical Co.). To ensure that equal amounts of proteins were loaded in the gel, silver staining was performed using the Silver Staining kit from Amersham Pharmacia Biotech. This visualization technique has a sensitivity of 0.2 ng protein/band and is 100 times more sensitive than conventional Coomassie blue staining. Proteins were separated on an SDS-6% polyacrylamide gel at 40 V overnight. Separated proteins were transferred onto an activated piece of polyvinylidine difluoride membrane (Immobilon-P; Millipore) at 200 mA for 40 min. The membrane was blocked with a buffer containing 5% milk powder, 20 mM Tris-HCl (pH 7.50), 150 mM NaCl, and 0.05% Tween 20 for 1 h followed by three washes with Tris-buffered saline-Tween (TBS-T). For Western blot analysis, membranes were incubated with the primary monoclonal antibody (rabbit anti-NOS 3 IgG; Santa Cruz Biotechnology, Inc.) in a dilution of 1:1,000 at room temperature for 2 h. After washing, incubation with the secondary antibody (peroxidase-labeled anti–rabbit IgG, 1:1,000; Amersham Pharmacia Biotech) followed at room temperature for 90 min. A control sample of human vein endothelial cells was run in parallel as a positive control. Prestained markers (Bio-Rad Laboratories) were used for molecular mass determinations. eNOS protein was finally detected by enhanced chemiluminescence (ECL; Amersham Pharmacia Biotech), and films were exposed for 15 s.

Determination of Fractionated eNOS Protein Expression

Frozen aortic segments (5 mm length) were pulverized and homogenized in a buffer (pH 7.40) containing 250 mM Tris-HCl, 10 mM EDTA, and 10 mM EGTA. After centrifugation at 21,000 *g* and 4°C for 5 min, the supernatant was transferred to fresh microcentrifuge tubes. NOS in soluble and membrane-associated fractions was separated by further centrifuging at 100,000 *g* for 60 min. The supernatant contains soluble NOS, whereas the pellet, which is resuspended in homogenization buffer, contains membrane-associated NOS. SDS-PAGE and Western blotting were performed as described for total eNOS protein expression. Films were exposed overnight.

NOS Activity Assay

Frozen aortic rings (5 mm length) were homogenized in 400 μl of a buffer containing 20 mmol/liter Hepes, 200 mmol/liter sucrose, 1 mmol/liter dithiothreitol, 10 μg/ml soybean trypsin inhibitor, 10 μg/ml leupeptin, and 2 μg/ml aprotinin. Before sonication, PMSF at 0.1 mmol/liter final concentration and [(3-cholamidopropyl)-dimethyl-ammonio]-1-propanesulfonate (CHAPS; 20 mmol/liter) were added to homogenized samples. Tissue homogenates of each age group of animals were pooled according to protein content, and samples were measured in triplicates. Samples were then centrifuged at 45,000 rpm and 4°C for 20 min. The supernatants were depleted of endogenous arginine by passage over activated resin, and the protein concentration was adjusted to 2.4 mg/ml. NOS activity was measured by the conversion of L-[^{14}C]arginine to L-[^{14}C]citrulline and expressed as pmol per μg protein per min (28). Cytosols from homogenized samples (18 μl) were incubated at 37°C for 20 min with 100 μl of the optimized assay buffer for citrulline formation consisting of: L-citrulline (1.2 mmol/liter), L-arginine (2×10^{-2} mmol/liter), NADPH (0.12 mmol/liter), tetrahydrobiopterin (10^{-2} mmol/liter), $MgCl_2$ (1.2 mmol/liter), $CaCl_2$ (0.24 mmol/liter), calmodulin (40 U/ml), FAD (10^{-3} mmol/liter), FMN (10^{-3} mmol/liter), and L-U[^{14}C]arginine (1.2×10^{-4} mmol/liter; 18.5 kBq/ml). Incubations were performed for each sample in the presence or absence of 1 mmol/liter EGTA to determine the amount of Ca^{2+}-dependent and Ca^{2+}-independent formation of citrulline. The NOS-specific and NOS-unspecific formation of citrulline was determined in samples containing 1 mmol/liter L-NMMA. The reaction was terminated by removal of substrate and addition of 1 ml (1:1, vol/vol) H_2O/Dowex 50 × 8-400 cationic resin, pH 7.20, and 5 ml of water. After centrifugation of the incubation mix for 3 min at 1,500 rpm, 4 ml supernatant in 10 ml scintillant was examined for [^{14}C]citrulline formation using a scintillation counter.

MnSOD Protein Expression

Extraction. Aortic segments of 5 mm length were snap frozen in liquid nitrogen immediately upon isolation. For SOD determination, aortas were homogenized and lysed in 200 μl Tris-SDS (2%) buffer. After 1 h of incubation on ice and 4 min of sonication in a water bath, the suspension was boiled for 2 min and the lysate centrifuged at 10,000 *g* at 4°C for 10 min. Protein concen-

tration measurement and silver staining were performed as described above.

Immunoprecipitation of MnSOD. 25 μl (~5 μg) solubilized protein was diluted in 1 ml TBS (pH 7.50) and incubated with 10 μl primary antibody (rabbit anti-MnSOD IgG; room temperature, 2 h; StressGen Biotechnologies) with mixing by end over end inversion. Immune complexes were precipitated with Protein G Plus Agarose (Santa Cruz Biotechnology Associates, Inc.) after incubation with mixing at room temperature for 4 h and centrifugation at 2,500 rpm (4°C, 5 min). After washing once in Tris saline azide (TSA, pH 8.0; 10 mM Tris, 140 mM NaCl, 0.025% NaN_3) twice in APS-SDS Triton X-100, and once in 50 mM Tris-HCl (pH 6.80), immunoprecipitated proteins were diluted in sample buffer and boiled for 10 min. After centrifugation at 10,000 rpm (room temperature, 1 min), the supernatant was loaded on SDS-PAGE.

Western Blot Analysis of MnSOD. Proteins were separated on 15% SDS-polyacrylamide gels at 40 V overnight and transferred electrophoretically onto polyvinylidine difluoride membranes (Immobilon-P; Millipore) at 200 mA for 40 min. Membranes were blocked with blocking buffer (as described above) for 1 h. For detection of MnSOD, membranes were incubated with the primary antibody (polyclonal rabbit anti-MnSOD IgG, dilution 1:2,000; StressGen Biotechnologies) at room temperature for 90 min. Nitrotyrosine-containing immunoprecipitated MnSOD was detected by incubating membranes at room temperature for 90 min with a rabbit polyclonal IgG antinitrotyrosine antibody (dilution 1:2,000; Upstate Biotechnology). After three washes in TBS-T, MnSOD membrane and immunocomplexes of MnSOD and nitrotyrosine were incubated at room temperature for an additional 90 min with a peroxidase-labeled anti–rabbit antibody (Amersham Pharmacia Biotech). Membranes were washed three times in TBS-T, and proteins were detected using enhanced chemiluminescence (ECL; Amersham Pharmacia Biotech). Films were exposed for 15 s to 3 min both for nitrotyrosine-containing MnSOD and for MnSOD.

Determination of Inducible NOS Protein Expression

For inducible NOS (iNOS) determination, extraction was performed as described above for MnSOD. Western blot analysis was performed as described above for eNOS protein expression. The primary monoclonal antibody (mouse anti-iNOS IgG; Transduction Laboratories) was used in a dilution of 1:2,000, the secondary antibody (peroxidase-labeled anti–mouse IgG; Amersham Pharmacia Biotech) in a dilution of 1:4,000. The positive control for iNOS was a mouse macrophage lysate (Transduction Laboratories).

For all the molecular biology techniques, homogenates of all animals belonging to one age group (young, $n = 8$; middle-aged, $n = 7$; or old, $n = 8$) were pooled according to protein content. Protein concentrations in the lysates were measured, and silver staining was performed to ensure that exactly the same amounts of protein were loaded in the gels. All experiments were performed at least three times and, unless otherwise stated, results from one representative experiment are shown.

Quantification of Blots

Blots were densitometrically quantified using the public domain NIH Image 1.60 program developed at the National Institutes of Health (available at http://rsb.info.nih.gov/nih-image/). In brief, after calibration of optical density, a density profile plot

Table I. *Comparison of Different Parameters in Young, Middle-aged, and Old Rats*

Parameter	Young	Middle-aged	Old	Significance level
Weight (g)	305 ± 8*	537 ± 7*	514 ± 20*	*$P < 0.0001$ for Y vs. M and Y vs. O
Systolic RR (mmHg)	121 ± 4	117 ± 4	117 ± 2	NS
Heart rate (bpm)	334 ± 13	323 ± 14	344 ± 13	NS
Maximal relaxations (%)				
Ach	−96 ± 2*	−89 ± 2*	−62 ± 3*	*$P < 0.0001$ for Y vs. O and M vs. O
A23187	−76 ± 1*	−74 ± 4*	−47 ± 4*	*$P < 0.0001$ for Y vs. O and M vs. O
SNP	−111 ± 2	−107 ± 1	−105 ± 1	NS
Maximal NO release (nmol/liter)	690 ± 50*	490 ± 70*	200 ± 30*	*$P < 0.0001$ for Y vs. O *$P < 0.001$ for M vs. O *$P < 0.01$ for M vs. Y
NOS activity (pmol/min/mg)				
Total	120 ± 13*	−	216 ± 26*	*$P < 0.01$
eNOS	23 ± 10**	−	144 ± 14**	**$P < 0.001$
iNOS	97 ± 15	−	72 ± 12	NS
Superoxide (cpm/mg dry wt)				
Basal	2,302 ± 323*	2,145 ± 220*	6,058 ± 445*	*$P < 0.0001$ for Y vs. O and M vs. O
Stimulated	82,495 ± 6,033**	108,439 ± 2,612	175,058 ± 36,080**	**$P < 0.01$

Y, young; M, middle-aged; O, old; RR, blood pressure; bpm, beats per minute.

was generated for each band. Base lines and drop lines were drawn manually so that each peak defined a closed area. The area beneath the peaks was electronically calculated and expressed as pixel intensity per unit area. Determinations of optical density were performed on each band of at least three different blots.

Preparation of Tissue for Immunoelectron Microscopy

Two additional young and two additional old F1 rats belonging to the cohorts from which the animals for all other experiments had been chosen were used for immunoelectron microscopy. The aorta was isolated as described above and immediately immersed into 4% formaldehyde (freshly prepared from paraformaldehyde) in PBS (room temperature). Using an infusion pump, the aorta was then perfused with the fixative at a constant flow rate of 1.5 ml/min for 30 min. After two washes in PBS, the aorta was kept in PBS containing 0.1% formaldehyde until further processing for microscopy.

Immunoelectron Microscopy

Tissue was processed as described previously (29). In brief, segments of aorta were cryoprotected with 30% polypropylene glycol and quench frozen in melting propane cooled in liquid nitrogen. They were freeze substituted against 0.1% uranyl acetate in methanol and embedded in Lowicryl HM20 at −50°C using a Reichert automatic freeze-substitution unit (Leica). Thin sections (50–60 nm) were cut using a Reichert Ultracut S ultramicrotome (Leica), and mounted on carbon Formvar-coated nickel grids. Sections were incubated with a 1:1,000 dilution of monoclonal mouse antibody against nitrotyrosine (Upstate Biotechnology). Control sections were incubated with either preimmune serum at 1:100 dilution or monoclonal mouse anti–human von Willebrand factor (1:25). All incubations were done at 4°C for 18 h. Primary antibody binding sites were visualized with goat anti–mouse IgG (H plus L)/10-nm gold conjugates (1 h, 4°C; British BioCell International). Sections were viewed with a CM100 transmission electron microscope (Philips).

Calculations and Statistical Analysis

When applicable (comparison between two values), statistical analysis was done by Student's *t* test. For multiple comparisons, results were analyzed by analysis of variance followed by Bonferroni's and Dunn's correction (30). Data are presented as means ± SEM. Means were considered significantly different at $P < 0.05$.

Results

Weight, Heart Rate, and Blood Pressure. Body weight was higher in old and middle-aged rats than in young rats. Systolic blood pressure and heart rate were not significantly different between the three groups (Table I).

Age-dependent Impairment of NO-mediated Vascular Endothelial Function. In old rats, NO-mediated, endothelium-dependent relaxation to acetylcholine was markedly reduced compared with young and middle-aged rats (Fig. 1 A, and Table I). Furthermore, aging was also associated with comparable reductions of NO-mediated, endothelium-dependent relaxation to the calcium ionophore A23187 (Fig. 1 B, and Table I). In contrast, there was no impairment of endothelium-independent relaxation to SNP in aged animals (Fig. 1 C, and Table I).

Age-associated Upregulation of the eNOS Enzyme System. Fig. 2 A depicts typical amperograms for each age group of direct in situ ex vivo measurements of NO on the aortic

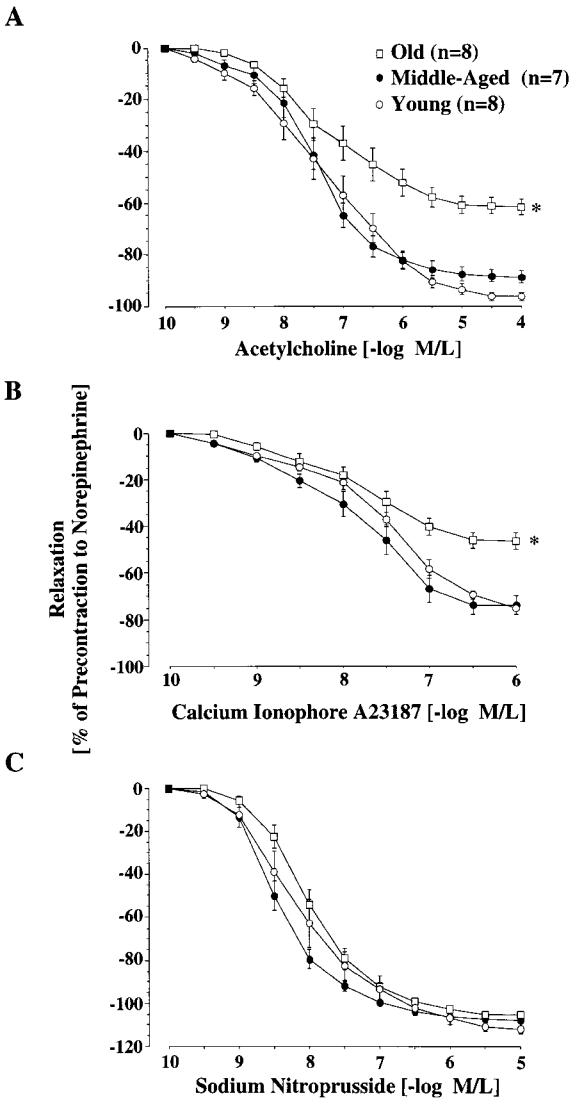

Figure 1. Age-dependent changes in endothelium-dependent and -independent relaxation of the rat aorta. Line graphs showing concentration–response curves to acetylcholine (A), calcium ionophore A23187 (B), and SNP (C). Relaxation to both endothelium-dependent agonists was reduced in old aortas ($P < 0.0001$). Endothelium-independent relaxation was unaffected by age. M/L, mol/liter.

endothelial surface after maximal stimulation with A23187 (10^{-6} M). A receptor-independent agonist was chosen for stimulation in order to delineate changes of eNOS activity rather than possible age-associated changes of receptor-mediated signal transduction. The porphyrinic microsensor, with its fast response time (0.1–10 ms), high sensitivity for NO, and lack of sensitivity to secondary species such as nitrate/nitrite, was chosen to provide the most precise, direct measurements of endogenous NO (25). Maximal NO levels were lower in aortas obtained from old and middle-aged animals compared with those from young rats (Fig. 2, and Table I).

As NO in vascular endothelial cells is synthesized by eNOS, we investigated the possibility that age-dependent

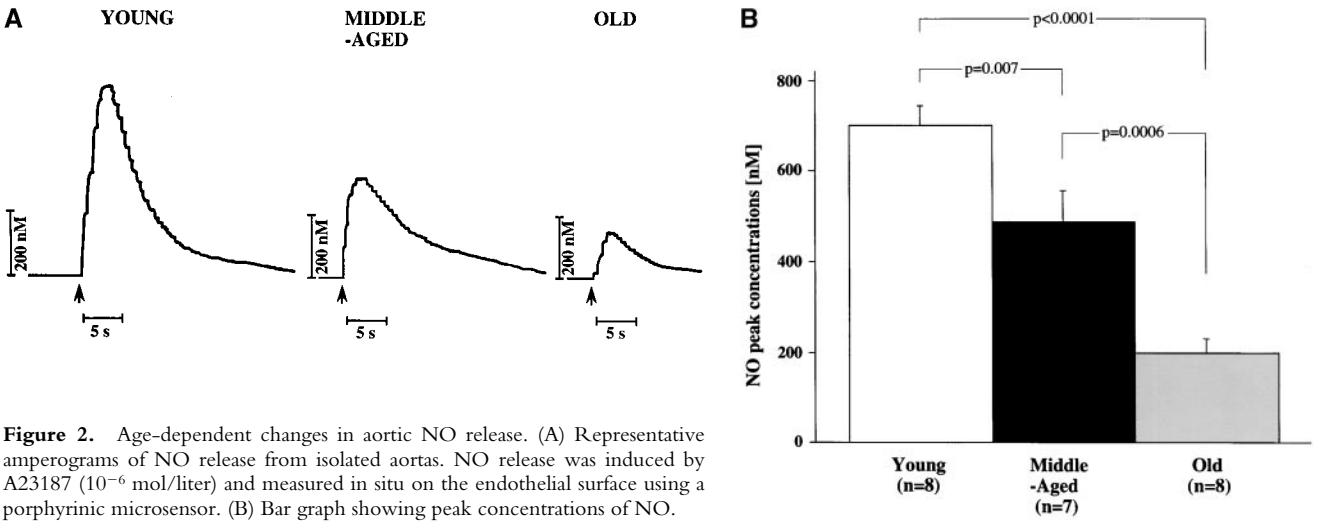

Figure 2. Age-dependent changes in aortic NO release. (A) Representative amperograms of NO release from isolated aortas. NO release was induced by A23187 (10^{-6} mol/liter) and measured in situ on the endothelial surface using a porphyrinic microsensor. (B) Bar graph showing peak concentrations of NO.

changes might be related to alterations in the expression and/or activity of the eNOS enzyme system. To this end, we determined eNOS protein expression selectively in homogenates of endothelium using a new extraction method. Strikingly, we found that eNOS protein expression steeply increased in an age-dependent manner, nearly sevenfold in old rats compared with young ones (Fig. 3) and nearly threefold in middle-aged animals (young versus old, middle-aged versus old, and young versus middle-aged; $P < 0.0001$). The age-dependent increase in eNOS expression was in sharp contrast to the decrease in NO detection. In contrast to eNOS, there was no iNOS expression detectable in all age groups (data not shown).

Analysis of the subcellular distribution of eNOS protein expression revealed that, in all age groups, eNOS was exclusively associated with the particulate, subcellular membrane fraction (Fig. 4 A) containing the biological activity of the enzyme (6, 7). No eNOS was found in the cytosolic fraction.

To confirm that eNOS overexpression was also associated with a higher activity, we determined eNOS activity by the conversion of L-[^{14}C]arginine into L-[^{14}C]citrulline.

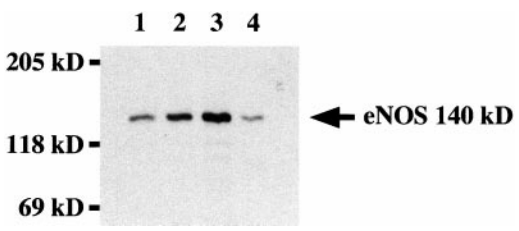

Figure 3. eNOS expression in rat aorta. Homogenates of aortic endothelium from young (lane 1), middle-aged (lane 2), and old (lane 3) rats were separated by SDS-PAGE and analyzed by Western blotting for eNOS expression. The position of the molecular mass markers is indicated (expressed in kD). Human umbilical vein endothelial cells (lane 4) were used as positive control.

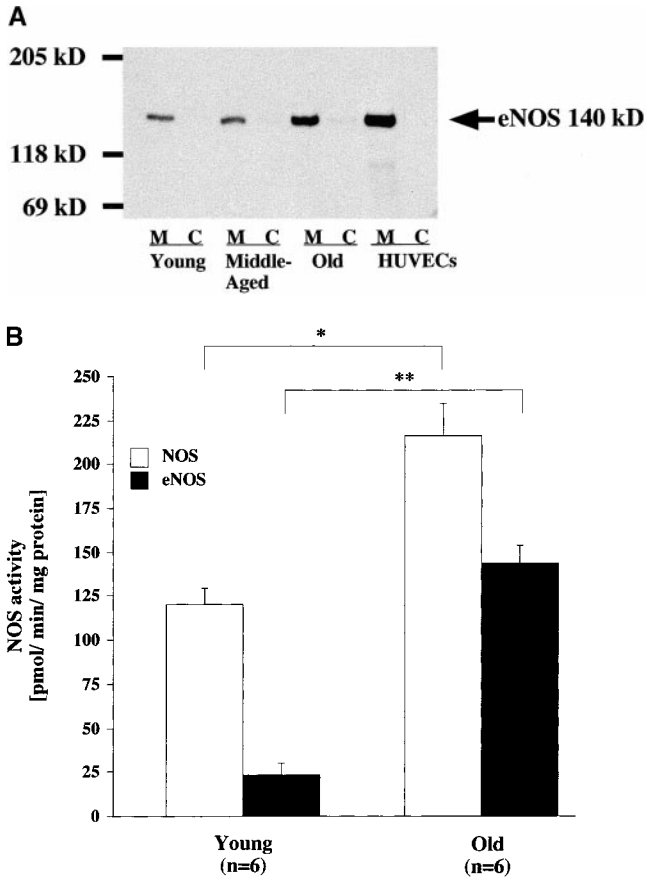

Figure 4. (A) Subcellular analysis of eNOS as detected by immunoblotting. Membrane-associated (M) and cytosolic (C) eNOS expression. Cytosolic and membrane fractions were prepared from homogenates of each age group and analyzed by immunoblotting. Data are representative of three experiments. HUVECs, human umbilical vein endothelial cells. (B) Activity of total NOS and eNOS in aortas from young and old rats. Activity was measured in homogenates of aortic tissue by determination of the rate of conversion of L-[^{14}C]arginine to L-[^{14}C]citrulline. Significance: total NOS, $*P < 0.01$; eNOS, $**P < 0.001$.

Using this test we found that both total NOS activity and eNOS activity were significantly greater in old than in young rats (Fig. 4 B, and Table I). The sevenfold increase in eNOS activity in old aortas parallels the increase in enzyme expression. In conclusion, fully active eNOS is upregulated with age, although the bioavailability of its intended product, NO, is significantly diminished. However, citrulline formation may not be stoichiometrically related to NO production, as a partial conversion of NOS to its oxidase form will also yield L-citrulline as an end product (31).

Age-associated Increased Vascular Superoxide Formation. $\cdot O_2^-$ is the main oxidant for NO (32). Therefore, we investigated the possibility that increased tissue levels of $\cdot O_2^-$ might be the cause of the inactivation of NO. Using a lucigenin enhanced chemiluminescence method, we found a threefold increase of basal and a twofold increase of stimulated (A23187 10^{-6} mol/liter) $\cdot O_2^-$-generated chemiluminescence in old aortas compared with young ones (Fig. 5 A, and Table I). This assay, in the absence of added NADH, largely reflects $\cdot O_2^-$ production.

To identify the source of $\cdot O_2^-$, aortic rings were mechanically denuded. Thereafter, $\cdot O_2^-$-generated chemiluminescence fell from 6,058 ± 445 to 2,293 ± 625 cpm/mg ($P = 0.02$), suggesting that the endothelium is the primary source of $\cdot O_2^-$ generation (Fig. 5 B). Values for young denuded aortas (3,019 ± 835 cpm/mg) did not significantly differ from those obtained from young aortas with an intact endothelium (2,302 ± 323 cpm/mg; NS). This suggests that in young aortas there is only a low, basal production of superoxide and also that the age-associated increase in $\cdot O_2^-$ occurs within the endothelium.

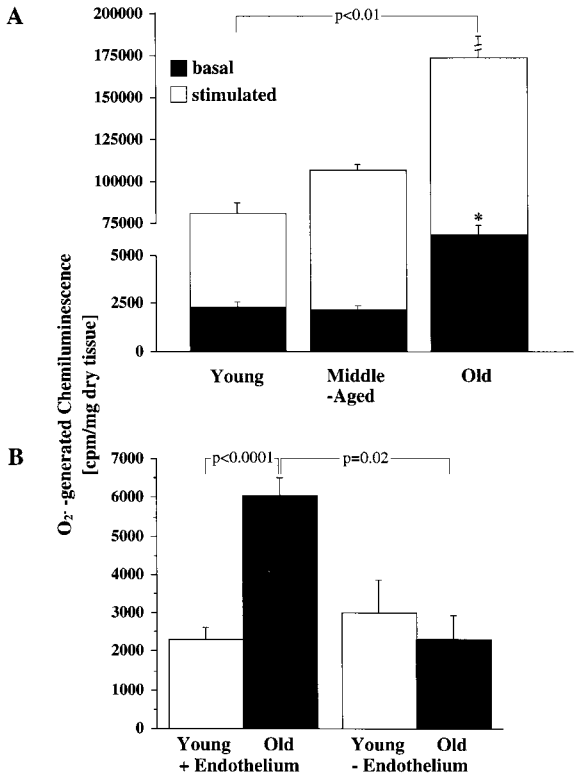

Figure 5. Age-dependent $\cdot O_2^-$ production. (A) Bar graph showing both basal amount of chemiluminescence generated by $\cdot O_2^-$ in aorta from young, middle-aged, and old rats (*$P < 0.0001$ versus basal values for young and middle-aged rats) and maximal generation of chemiluminescence after stimulation with calcium ionophore A23187 (10^{-6} mol/liter). (B) The influence of endothelium: aortic rings from young and old ($n = 6$ each) rats were mechanically denuded, and the basal chemiluminescence signal was compared with that from intact aortas.

Increased Vascular Deposition of 3-Nitrotyrosinated Proteins in Distinct Cellular and Subcellular Compartments of the Vasculature. We then sought to prove that peroxynitrite was indeed formed after the capture of NO by $\cdot O_2^-$ in the aging vasculature and, if so, to clarify its biological effects on antioxidative enzymes. Therefore, we studied the distribution of 3-nitrotyrosine residues, which are typical end products of the reaction of peroxynitrite with biological compounds. As shown in Fig. 6, aortic tissue sections from old animals exhibited a markedly increased specific immunostaining with a monoclonal antibody to nitrotyrosine compared with young animals. In the endothelium of old aortas (Fig. 6 A), significant amounts of nitrotyrosine accumulated in the nucleus, the cytosol, and the mitochondria compared with young aortas (Fig. 6 B). The extracellular matrix of the intima (Fig. 6 E) and vascular smooth muscle cells within the media (Fig. 6 G) of old aorta also had an enhanced immunolabeling compared with young tissue (Fig. 6, D and F, respectively). Quantification of immunogold labeling for nitrotyrosine is shown in Fig. 7, A and B. Depending on the subcellular compartment examined, a two- to sixfold increased labeling of old aorta was observed. A particularly high labeling density for nitrotyrosine was found in the mitochondria of endothelial cells. It is of importance to note that these vessels do not exhibit any particular signs of atherosclerosis, as confirmed by electron microscopy.

Increased Nitration of MnSOD as a Molecular Marker for Age-associated Mitochondrial Oxidative Stress in the Vasculature. Immunoelectron microscopy strongly supported that the most significant generation of oxidants, namely $\cdot O_2^-$ and peroxynitrite, occurs within the mitochondria and in particular, in those within the endothelium. This is of particular interest as, in a different pathophysiological context, the nitration and inactivation of mitochondrial MnSOD had been reported (22). Therefore, it was considered important that the effect of aging on this mitochondrial enzyme was analyzed further. Surprisingly, immunoblot analysis of aortic homogenates from different age groups with polyclonal anti-MnSOD antibody revealed no significant change in enzyme expression (Fig. 8 A). We then confirmed nitration of tyrosine residues in MnSOD by immunoblot analysis of MnSOD, which had been immunoprecipitated from aortic tissue with a polyclonal anti-MnSOD antibody. Indeed, immunodetection with polyclonal anti-nitrotyrosine antibody showed increased levels of tyrosine-nitrated MnSOD in old and middle-aged aortas compared with young ones (Fig. 8 B). Densitometric analysis of the Western blots showed that nitration of MnSOD significantly increased with age in old aortic tissue (Fig. 8 C). To

ensure that the same amounts of protein were loaded, a silver staining was performed before each Western blot analysis (not shown).

Discussion

This study provides new insights into the mechanisms of endothelial dysfunction that occur with age and offers a coherent picture of the underlying biochemical events. In agreement with previous reports, we found that detectable levels of NO were clearly reduced with age but, for the first time, we demonstrate that decreased NO production is a consequence neither of a reduced expression of the NO-producing enzymes nor of a reduced activity in the L-arginine/NO pathway, as both are sevenfold higher in aged compared with young aortas. As this was accompanied by a threefold higher activity in endothelial $\cdot O_2^-$ production, the age-associated, decreased endothelial NO levels, and hence impaired vascular relaxation, must be a consequence of the known rapid reaction between the two radicals. The resulting formation of peroxynitrite is confirmed by enhanced vascular nitration. The conclusion that NO must be inactivated by $\cdot O_2^-$ is supported by three observations: (a) in the old aorta, reduced NO levels occur in the presence of increased eNOS expression and activity; (b) increased $\cdot O_2^-$ levels with aging occur concomitantly with decreased NO levels; and (c) $\cdot O_2^-$ rapidly reacts with NO to form peroxynitrite, and this reaction is reflected by tyrosine nitration in proteins such as MnSOD.

Based on these new findings, we hypothesize an age-related gradual change in a distinct network of different signals, including up- and/or downregulation which controls vascular function. Mitochondria and an increased one-electron oxidation of respiratory chain components may be involved in the initial reactions. As a consequence, the protective mechanisms that preserve endothelial function are dramatically "switched on" (i.e., upregulation of the eNOS enzyme system), but the balance between vascular protec-

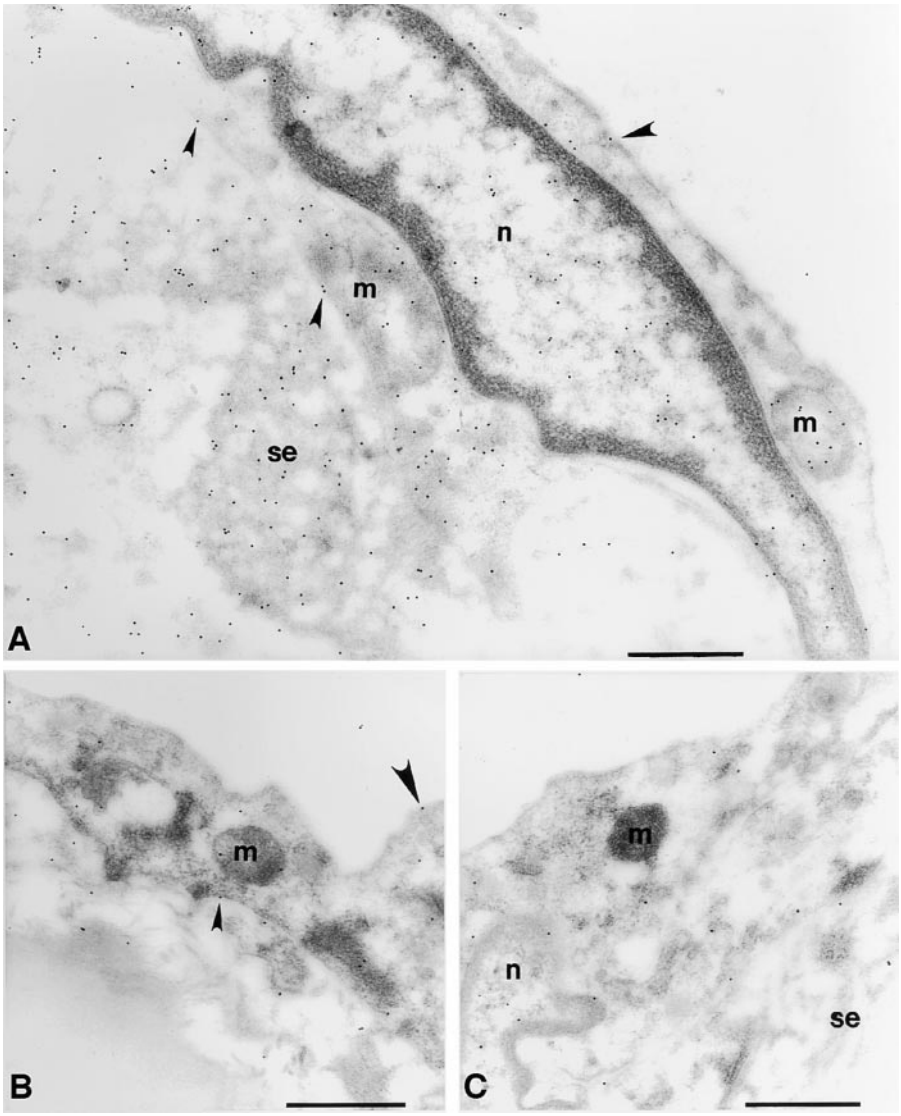

Figure 6. The accumulation of 3-nitrotyrosine is increased in the aorta of the old rat compared with that of the young rat. Representative electron micrographs show the pattern of immunogold labeling for 3-nitrotyrosine in thin sections of young (B, D, and F) and old (A, E, and G) aortas. Primary antibody binding sites were visualized with goat anti–mouse IgG conjugated to 10-nm gold particles. (A) Intima of the aorta from an old rat. Label is densest over mitochondria (m) and strong over nucleoplasm (n) and over endothelial cell cytoplasm. Sparse labeling is associated with the luminal plasmalemma (large arrowheads) and stronger label is present over the abluminal plasmalemma (small arrowheads). Strong labeling is seen in the subendothelial space (se). (B) Intima of the aorta from a young rat. Label is lower over mitochondria and cytoplasm and sparse over the luminal plasmalemma (large arrowhead) and the abluminal plasmalemma (small arrowhead). (C) Intima of an old rat. The primary antisera against nitrotyrosine was preincubated with 20 μmol/liter nitrotyrosine for 1 h before labeling as in A and B. Label density is reduced to levels lower than those seen in the young rats in all compartments.

tion and damage cannot be preserved, as it is in young animals. As the functional responses to the receptor-dependent and -independent endothelium-dependent vasodilators acetylcholine and A23187, respectively, were superimposable, age-associated endothelial dysfunction is not related to an alteration of the signal transduction pathway, but instead to reduced bioavailability of NO.

Paradoxically, both eNOS protein expression and L-arginine turnover were increased sevenfold in aortas from old animals. Previous work demonstrated a marginal increase in eNOS protein expression, but not activity, in the aorta of 20-mo-old male Wistar rats (9). The increase described here is much more dramatic and might be due to the considerably higher age of the animals used in this study and to our new technique for the isolation of vascular endothelium. In addition, we found that eNOS activity was similarly increased, demonstrating the functional integrity and in fact overactivity of the L-arginine/NO pathway even at extreme age. This conclusion is further strengthened by the subcellular distribution of eNOS. Association of eNOS with the cell membrane determines the biological activity of the enzyme, and its location in caveolae may facilitate NO signaling to adjacent smooth muscle cells (7). It is likely that the eNOS enzyme system is overactivated in aged blood vessels as a compensatory mechanism to counterbalance endothelial dysfunction induced by age-dependent oxidative stress. Another reason for increased eNOS expression might be hemodynamic forces such as shear stress, which have been shown to upregulate eNOS in vitro (33). However, neither blood pressure, heart rate, nor hematocrit value changed with age in these animals. In contrast to eNOS, there was no significant difference in both iNOS activity and expression between young and old animals, suggesting that iNOS does not contribute to the compensatory mechanism of NOS upregulation.

The major and crucial finding of this study is the markedly increased $\cdot O_2^-$ production (most of which was derived from the endothelium) with aging. The use of lucigenin to detect $\cdot O_2^-$ in tissue has recently become a subject

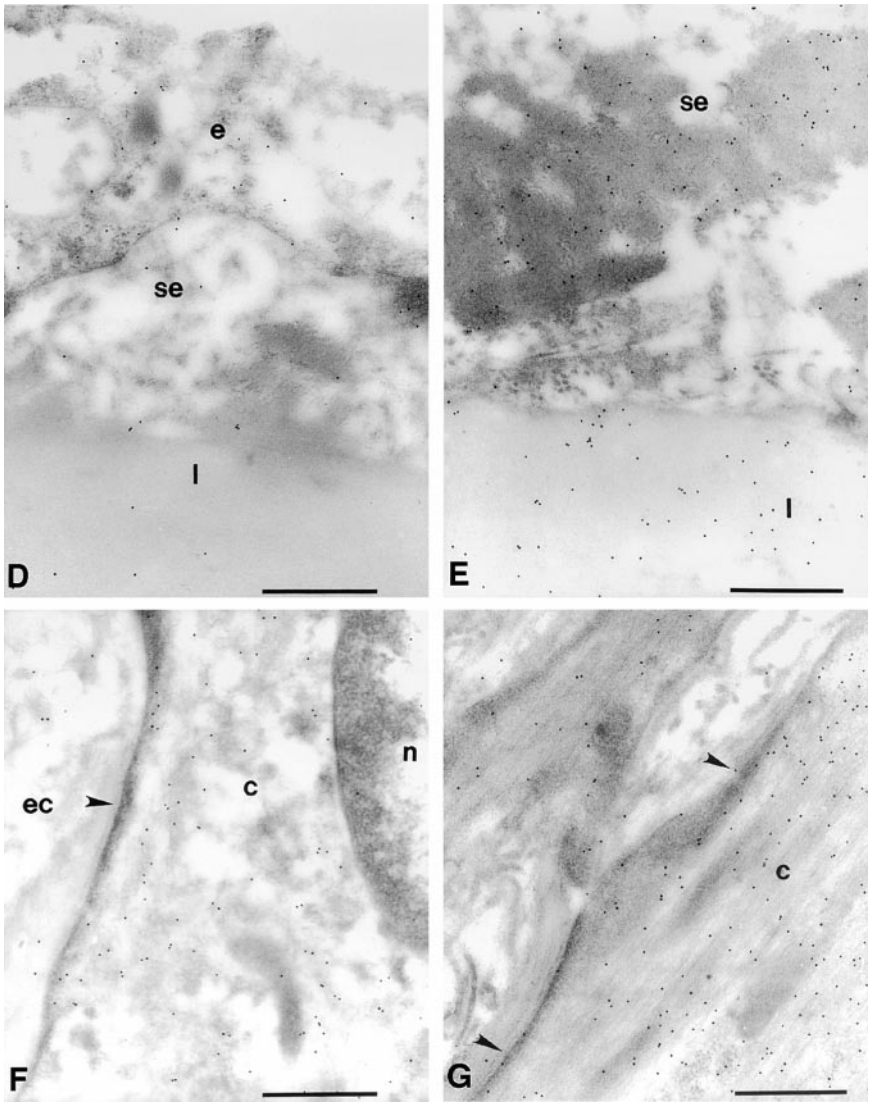

Figure 6. continued.

(D) Intima of a young rat showing low levels of labeling over the endothelium (e) and sparse labeling over the subendothelial space and the first elastic lamellae (l). (E) Subendothelial space and the first elastic lamellae of an old rat. Labeling density is much greater in both compartments and is particularly dense over aggregates of electron dense material seen in the subendothelial space. (F) Smooth muscle cell in the medial layer of the aorta of a young rat. Label is strongest over the cytoplasm (c) and low over the nucleoplasm and extracellular space (ec) and seldom seen over the sarcolemma (arrowhead). (G) Smooth muscle cell in the medial layer of the aorta from an old rat. Labeling is much stronger over the cytoplasm and is frequently seen over the sarcolemma (arrowheads). Bars, 0.5 μm. Original magnifications: ×22,000.

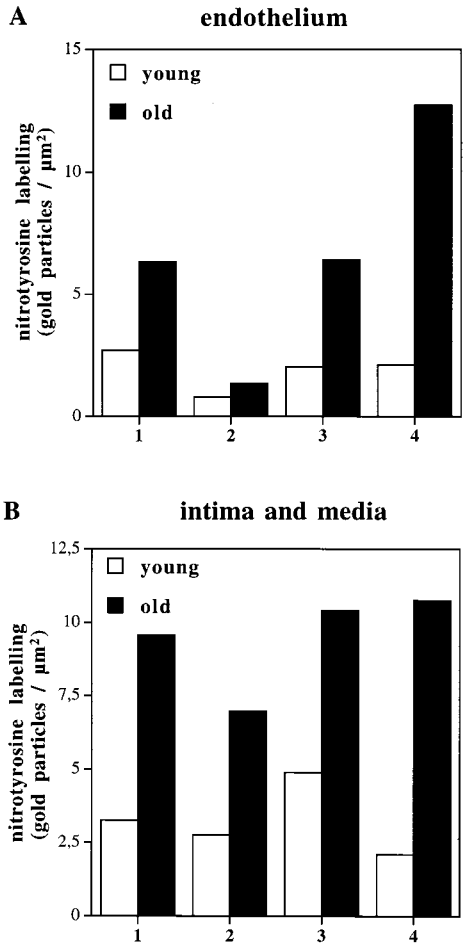

Figure 7. Quantitative analysis of immunogold labeling for 3-nitrotyrosines in young and old aortas in endothelium (A) and intima/media (B). Two sections were prepared from randomly selected areas of each aorta (see Materials and Methods). On each section, 15 fields of endothelium, intima, and media were randomly chosen. In each area of endothelium, immunogold labeling density was estimated over heterochromatin (1), euchromatin (2), cytosol (3), and mitochondria (4). In the intima, immunogold labeling was also estimated over the subendothelial space (1) and the elastic lamellae (2). In the media, immunogold labeling density was estimated over the cytosol (3) and mitochondria (4). All data are presented as means of the labeling density in each region of each of two sections from each aorta.

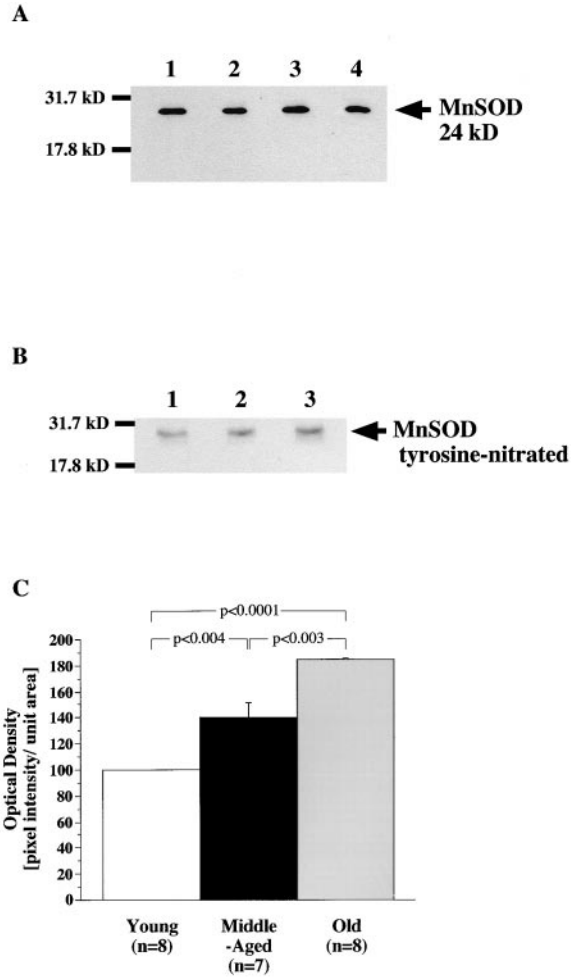

Figure 8. Total protein expression and age-associated increased nitration of mitochondrial MnSOD. Western blot of MnSOD (A) from young (lane 1), middle-aged (lane 2), and old (lane 3) aortas. Extracted proteins were separated on 15% SDS-PAGE gels and examined by Western blot with a polyclonal antibody against MnSOD. Recombinant MnSOD served as a positive control (lane 4). Molecular weight markers are indicated (in kD) on the left. (B) Nitrotyrosine-containing immunoprecipitated MnSOD from young (lane 1), middle-old (lane 2), and old (lane 3) rats were separated by 15% SDS-PAGE gels and analyzed by Western blot with a polyclonal antibody against nitrotyrosine. Films were exposed for 15 s to 3 min. (C) Quantitative analysis of tyrosine-nitrated MnSOD.

of controversy, as lucigenin may itself enhance $\cdot O_2^-$ formation (34, 35). However, if autoxidation of lucigenin had in part contributed to $\cdot O_2^-$ generation, this would have been applicable to the same extent to all age groups and would not affect the relative differences observed.

The increased $\cdot O_2^-$ production led to an inactivation of equimolar amounts of NO by the formation of peroxynitrite, which, in turn, exhibits new messenger functions. The highest density of immunogold labeling for 3-nitrotyrosyl was found in the mitochondria, in particular in those within the endothelium, indicating that nitrotyrosination was dominant in these organelles and supporting their importance in the cascade of events contributing to the aging process. This may well have distinct pathophysiological consequences. Although we did not directly investigate mitochondria, it is reasonable to assume that mitochondria themselves may be a major source of $\cdot O_2^-$ and peroxynitrite in the aging vascular system (36). Autoxidation of components of the respiratory chain would lead to the formation of $\cdot O_2^-$, which is the one-electron reduction product of oxygen. Increased $\cdot O_2^-$ production is unsuccessfully counter-balanced by the enhanced expression and activity of NO-synthesizing enzymes. At least in the chronic process of vascular aging, this directly involves eNOS but not iNOS, although in situations of acute oxidative stress, iNOS may also be induced (37).

Peroxynitrite nitrates an essential tyrosine residue in Mn-SOD with the participation of manganese catalysis. In fact,

our results suggest that the nitration of tyrosine within MnSOD might be a mechanism leading to a significant reduction of its activity (38), and a possible further increase of $\cdot O_2^-$ formation. Nitration and dityrosine formation, both of which can easily be mediated by peroxynitrite, are both required to completely inhibit MnSOD. However, a partial inhibition of this crucial enzyme may also have important biological consequences (MacMillan-Crow, L.A., personal communication). MnSOD is the major antioxidant enzyme in the mitochondria of all mammals, and it is an endogenous nitration target in human renal allograft rejection (22). This study is the first to suggest that the degree of nitration of this enzyme may also be a molecular footprint of vascular aging. Proof for a pivotal role of MnSOD is provided by a recent report showing that genetic inactivation of MnSOD in mutant mice results in premature death (39), and that treatment with the SOD mimetic manganese–tetrakis-benzoic acid-porphyrin (MnTBAP) dramatically prolongs their survival. Manganese porphyrins also have a high capacity for the elimination of peroxynitrite (40). Our findings suggest that mitochondrial MnSOD may be a potentially important and novel drug target for the alleviation of vascular aging. It is of particular interest to the design of future therapeutic strategies to combat nitration-associated vascular aging to note that manganese porphyrins become even more efficient reductases for peroxynitrite when coupled with the biological antioxidants vitamin C, vitamin E, and glutathione, all of which serve as electron sources for the reduction of peroxynitrite (40).

Although 3-nitrotyrosyl labeling would be in line with a mitochondrial source of $\cdot O_2^-$, other sources, such as NADPH-oxidase (41), xanthin oxidase, or eNOS (42) itself, also have to be considered as contributors to $\cdot O_2^-$ and peroxynitrite formation. eNOS, in the absence of cofactors such as tetrahydrobiopterin, or in case of insufficient substrate supply, will exhibit oxidase activity (31). The dramatic increase in activity and expression of eNOS seen in the aged aorta may eventually not (or not only) be beneficial as an attempt by the organism to maintain endothelial function, but rather be detrimental, with eNOS becoming part of a redox system that increases electron transfer to oxygen. However, attempts to identify eNOS as the enzymatic source of $\cdot O_2^-$ will be hampered by the fact that selective inhibitors of its oxidase activity are not available to date. It remains to be determined whether eNOS plays a more pathological or a more protective role in vascular aging.

As eNOS expression and citrulline formation from L-arginine are dramatically increased with age, the diminished formation of free NO must be primarily a consequence of augmented $\cdot O_2^-$ generation. The link between increased $\cdot O_2^-$ production and decreased NO release is stringent in view of the known chemistry, kinetics, and diffusion properties of both free radicals. This reaction is currently accepted as the main biological source of peroxynitrite responsible for tyrosine nitration (43, 44). This would also be in agreement with our measurements of $\cdot O_2^-$ and nitrated proteins. Future work will be concerned with the identification of nitrotyrosinated prostacyclin synthase, the only other enzyme for which nitration by reaction with peroxynitrite and subsequent inactivation has been reported (45), and which has been associated with endothelial dysfunction in atherosclerosis (21) and ischemia-reperfusion damage (46).

The analysis presented here sets the basis for future studies in the field of vascular aging, in particular for those aimed at preventing age-related vascular dysfunction. Based on the knowledge of the mechanisms involved in the aging process of the endothelium, which is crucial to maintain normal vascular function, strategies to prevent this process should be designed and tested. New therapeutic interventions to prevent vascular aging might have enormous medical consequences given the strong age dependency of cardiovascular diseases.

The authors are indebted to S. Moncada, W.H. Koppenol, L.A. MacMillan-Crow, and M. Barton for most stimulating discussions, and to L.V. d'Uscio as well as L. Altwegg for assistance with statistical analysis. We furthermore thank C. Barandier, H. Greutert, and U. Moehrlen for expert technical assistance. The gold labeling was carried out in the Multi-Imaging Centre (Cambridge, UK), which was established, in part, with funding from the Wellcome Trust.

This work was supported in part by grants from the Swiss National Research Foundation (32-51069.97 and 32-49126.96), from Aetas, Foundation for Research into Ageing (Geneva, Switzerland), the Foundation Silva-Casa (Berne, Switzerland), and from the Swiss Heart Foundation. B. van der Loo was supported by fellowships from the European Society of Cardiology and the Roche Research Foundation (Basel, Switzerland). The Forschergruppe at the University of Konstanz was supported by a grant from the Deutsche Forschungsgemeinschaft.

Submitted: 24 July 2000
Revised: 9 October 2000
Accepted: 13 October 2000

References

1. Lüscher, T.F., and G. Noll. 1995. The endothelium in coronary vascular control. *Heart Dis.* 3:1–10.
2. Palmer, R.M., D.S. Ashton, and S. Moncada. 1988. Vascular endothelial cells synthesize nitric oxide from L-arginine. *Nature.* 333:664–666.
3. Moncada, S., and A. Higgs. 1993. The L-arginine-nitric oxide pathway. *N. Engl. J. Med.* 329:2002–2012.
4. Moncada, S. 1992. The 1991 Ulf von Euler Lecture. The L-arginine: nitric oxide pathway. *Acta Physiol. Scand.* 145: 201–227.
5. Pollock, J.S., U. Förstermann, J.A. Mitchell, T.D. Warner, H.H.W. Schmidt, M. Nakane, and F. Murad. 1991. Purification and characterization of particulate endothelium-derived relaxing factor synthase from cultured and native bovine aortic endothelial cells. *Proc. Natl. Acad. Sci. USA.* 88:10480–10484.
6. Sessa, W.C., C.M. Barber, and K.R. Lynch. 1993. Mutation of N-myristoylation site converts endothelial cell nitric oxide synthase from a membrane to a cytosolic protein. *Circ. Res.* 72:921–924.
7. Busconi, L., and T. Michel. 1993. Endothelial nitric oxide synthase. N-terminal myristoylation determines subcellular

localization. *J. Biol. Chem.* 268:8410–8413.
8. Tschudi, M.R., M. Barton, N.A. Bersinger, P. Moreau, F. Cosentino, G. Noll, T. Malinski, and T.F. Lüscher. 1996. Effect of age on kinetics of nitric oxide release in rat aorta and pulmonary artery. *J. Clin. Invest.* 98:899–905.
9. Cernadas, M.R., L. Sanchez de Miguel, M. Garcia-Duran, F. Gonzales-Fernandez, I. Millas, M. Monton, J. Rodrigo, L. Rico, P. Fernandez, T. de Frutos, et al. 1998. Expression of constitutive and inducible nitric oxide synthases in the vascular wall of young and aging rats. *Circ. Res.* 83:279–286.
10. Gryglewski, R.J., R.M. Palmer, and S. Moncada. 1986. Superoxide anion is involved in the breakdown of endothelium-derived vascular relaxing factor. *Nature.* 320:454–456.
11. Azhar, S., L. Cao, and E. Reaven. 1995. Alteration of the adrenal antioxidant defense system during aging in rats. *J. Clin. Invest.* 95:1414–1424.
12. Challah, M., S. Nadaud, M. Philippe, T. Battle, F. Soubrier, B. Corman, and J.B. Michel. 1997. Circulating and cellular markers of endothelial dysfunction with aging in rats. *Am. J. Physiol.* 273:H1941–H1948.
13. Harrison, D.G. 1997. Cellular and molecular mechanisms of endothelial cell dysfunction. *J. Clin. Invest.* 100:2153–2157.
14. Stadtman, E.R. 1992. Protein oxidation and aging. *Science.* 257:1220–1224.
15. Beckman, J.S., M. Carson, and W.H. Koppenol. 1993. ALS, SOD and peryoxynitrite. *Nature.* 364:584.
16. Koppenol, W.H. 1999. Chemistry of peroxynitrite and its relevance to biological systems. *In* Metal Ions in Biological Systems. Vol. 36. Interrelations between Free Radicals and Metal Ions in Life Processes. A. Sigel and H. Sigel, editors. Marcel Dekker Inc., New York. 597–619.
17. Marla, S.S., J. Lee, and J.T. Groves. 1997. Peroxynitrite rapidly permeates phospholipid membranes. *Proc. Natl. Acad. Sci. USA.* 94:14243–14248.
18. Beckman, J.S., H. Ischiropoulos, L. Zhu, M. van der Woerd, C. Smith, J. Chen, J. Harrison, J.C. Martin, and M. Tsai. 1992. Kinetics of superoxide dismutase and iron catalyzed nitration of phenolics by peroxynitrite. *Arch. Biochem. Biophys.* 298:438–445.
19. Haddad, I.Y., G. Patalli, P. Hu, C. Galliani, J.S. Beckman, and S. Matalon. 1994. Quantitation of nitrotyrosine levels in lung sections of patients and animals with acute lung injury. *J. Clin. Invest.* 94:2407–2413.
20. Zhou, M., C. Martin, and V. Ullrich. 1997. Tyrosine nitration as a mechanism of selective inactivation of prostacyclin synthase by peroxynitrite. *Biol. Chem.* 378:707–713.
21. Beckman, J.S., Y.Z. Ye, P.G. Anderson, J. Chen, M.A. Accavitti, M.M. Tarpey, and C.R. White. 1994. Extensive nitration of protein tyrosines in human atherosclerosis detected by immunohistochemistry. *Biol. Chem. Hoppe-Seyler.* 375:81–88.
22. MacMillan-Crow, L.A., J.P. Crow, J.D. Kerby, J.S. Beckman, and J.A. Thompson. 1996. Nitration and inactivation of manganese superoxide dismutase in chronic rejection of human renal allografts. *Proc. Natl. Acad. Sci. USA.* 93:11853–11858.
23. Leeuwenburg, C., P. Hansen, A. Shaish, J.O. Holoszy, and J.W. Heinecke. 1998. Markers of protein oxidation by hydroxyl radical and reactive nitrogen species in tissues of aging rats. *Am. J. Physiol.* 274:R453–R461.
24. Viner, R.I., D.A. Ferrington, A.F.R. Hühmer, D.J. Bigelow, and C. Schöneich. 1996. Accumulation of nitrotyrosine on the SERCA2a isoform of SR Ca-ATPase of rat skeletal muscle during aging: a peroxynitrite-mediated process? *FEBS Lett.* 379:286–290.
25. Malinski, T., and Z. Zaha. 1992. Nitric oxide release from a single cell measured in situ by a porphyrinic-based microsensor. *Nature.* 358:676–678.
26. Gyllenhammer, H. 1987. Lucigenin chemiluminescence in the assessment of neutrophil superoxide production. *J. Immunol. Methods.* 97:209–213.
27. Brandes, R.P., M. Barton, K.M.H. Philippens, G. Schweitzer, and A. Mügge. 1997. Endothelial-derived superoxide anions in pig coronary arteries: evidence from lucigenin chemiluminescence and histochemical techniques. *J. Physiol.* 500:331–342.
28. Knowles, R.G., and M. Salter. 1994. Measurement of NOS activity by conversion of radiolabeled arginine to citrulline using ion exchange separation. *In* Methods in Molecular Biology. Vol. 100. M.A. Titheradge, editor. Humana Press Inc., Totowa, NJ. 67–73.
29. Zajizek, J., M. Wing, J.N. Skepper, and A. Compston. 1995. Human oligodendrocytes are not sensitive to complement: a study of CD59 expression in the human central nervous system. *Lab. Invest.* 73:128–138.
30. Wallenstein, S., C.L. Zucker, and J. Fleiss. 1980. Some statistical methods useful in circulation research. *Circ. Res.* 47:1–9.
31. Vasquez-Vivar, J., N. Hogg, P. Martasek, H. Karoui, K.A. Pritchard, Jr., and B. Kalyansaraman. 1999. Tetrahydrobiopterin-dependent inhibition of superoxide generation from neuronal nitric oxide synthase. *J. Biol. Chem.* 274:26736–26742.
32. Dinerman, J., C. Lowenstein, and S. Snyder. 1993. Molecular mechanisms of nitric oxide regulation. Potential relevance to cardiovascular disease. *Circ. Res.* 73:217–222.
33. Ranjan, V., Z. Xiao, and S.L. Diamond. 1995. Constitutive NOS expression in cultured endothelial cells is elevated by fluid shear-stress. *Am. J. Physiol.* 269:H550–H555.
34. Tarpey, M.M., C.R. White, E. Suarez, G. Richardson, R. Radi, and B.A. Freeman. 1999. Chemiluminescent detection of oxidants in vascular tissue. Lucigenin but not coelenterazine enhances superoxide formation. *Circ. Res.* 84:1203–1211.
35. Liochev, S.I., and I. Fridovich. 1997. Lucigenin (bis-N-methylacridinium) as a mediator of superoxide anion production. *Arch. Biochem. Biophys.* 337:115–120.
36. Beckman, K.B., and B.N. Ames. 1998. Mitochondrial aging: open questions. *Ann. NY Acad. Sci.* 854:118–127.
37. Crespo, E., M. Macias, D. Pozo, G. Escames, M. Martin, F. Vives, J.M. Guerrero, and D. Acuna-Castroviejo. 1999. Melatonin inhibits expression of the inducible NO synthase II in liver and lung and prevents endotoxemia in lipopolysaccharide-induced multiple organ dysfunction syndrome in rats. *FASEB (Fed. Am. Soc. Exp. Biol.) J.* 13:1537–1546.
38. MacMillan-Crow, L.A., J.P. Crow, and J.A. Thompson. 1999. Peroxynitrite-mediated inactivation of manganese superoxide dismutase involves nitration and oxidation of critical tyrosine residues. *Biochemistry.* 37:1613–1622.
39. Melov, S., J.A. Schneider, B.J. Day, D. Hinerfeld, P. Coskem, S.S. Mirra, J.D. Crapo, and D.C. Wallace. 1998. A novel neurological phenotype in mice lacking mitochondrial manganese superoxide dismutase. *Nat. Genet.* 18:159–163.
40. Lee, J., J.A. Hunt, and J.T. Groves. 1998. Manganese porphyrins as redox-coupled peroxynitrite reductases. *J. Am. Chem. Soc.* 120:6053–6061.
41. Channock, S.J., J. El Benna, R.M. Smith, and B.M. Babior.

1994. The respiratory burst oxidase. *J. Biol. Chem.* 269: 24519–24522.
42. Cosentino, F., S. Patton, L.V. d'Uscio, E.R. Werner, G. Werner-Felmayer, P. Moreau, T. Malinski, and T.F. Lüscher. 1998. Tetrahydrobiopterin alters superoxide and nitric oxide release in prehypertensive rats. *J. Clin. Invest.* 101: 1530–1537.
43. Goldstein, S., G. Czapski, J. Lind, and G. Merenyi. 2000. Tyrosine nitration by simultaneous generation of NO and $\cdot O_2^-$ under physiological conditions. How the radicals do the job. *J. Biol. Chem.* 275:3031–3036.
44. Reiter, C.D., R.J. Teng, and J.S. Beckman. 2000. Superoxide reacts with nitric oxide to nitrate tyrosine at physiological pH via peroxynitrite. *J. Biol. Chem.* 275:32460–32466.
45. Zou, M., and M. Bachschmid. 1999. Hypoxia-reoxygenation triggers coronary vasospasm in isolated bovine coronary arteries via tyrosine nitration of prostacyclin synthase. *J. Exp. Med.* 190:135–138.
46. Liu, P., C.E. Hock, R. Nagele, and P.Y. Wong. 1997. Formation of nitric oxide, superoxide, and peroxynitrite in myocardial ischemia-reperfusion injury in rats. *Am. J. Physiol.* 272:H2327–H2336.